

Density-functional study of the pure and palladium doped small copper and silver clusters

Hamideh Kahnouji, Halimeh Najafvanzadeh *, S. Javad Hashemifar,[†] Mojtaba Alaei, and Hadi Akbarzadeh
Department of Physics, Isfahan University of Technology, 84156-83111 Isfahan, Iran

The size-dependent electronic, structural, magnetic and vibrational properties of small pure copper and silver clusters and their alloys with one and two palladium atoms are studied by using full-potential all-electron density functional computations. The stable isomers of these clusters are identified and their theoretical magic numbers are determined via the analysis of the second difference of their minimized energy. We discuss that the doped Pd atoms generally prefer to sit in the high coordination sites of the pure clusters. It is argued that Pd doping influences the structural properties and the two dimensional to three dimensional structural cross over in the small Cu and Ag clusters. The many body based GW correction is applied for more accurate determination of the electron affinity and ionization potential of these systems. Magnetic and vibrational properties of the pure and doped clusters are presented and discussed.

I. INTRODUCTION

Noble metal nanoclusters are currently attracting a great deal of attention within both experimental and theoretical communities, due to their interesting structural and electronic properties and promising technological applications in nano electronics, nano optics, biological sensing, catalysis, and biomedicine [1–5]. While transition metal ions may induce health and environmental problems [6, 7], noble metal nanoclusters exhibit lower toxicity and hence more biocompatibility. Noble metal nanoclusters are alloyed with palladium atoms to improve their catalytic activity [8, 9]. In recent years, extensive computational studies have been devoted to properties of pure noble metal clusters [10–13], although less information is available about structural and electronic properties of the corresponding bimetallics [14–16].

Among noble metal based bimetallic nanoclusters, copper and silver based nano-alloys have been studied considerably less than gold based bimetallic nanoclusters. Wang et al. [17] and Romanowski et al.[18] used density functional (DFT) computations to study AgPd and CuPd dimers and their interaction with H₂. Other calculations have been performed on Cu-Pd trimers and their interaction with molecular and atomic oxygen [19]. The stable geometry of small Ag_nPd_m clusters up to five atoms were found to transform from two-dimensional to three-dimensional as the Pd content increases [20]. Zhao et al. performed first-principles calculations to study the effects of Pd doping on structural and electronic properties of Ag_nPd ($n \leq 5$) clusters and their mono hydrides [21]. Efremenko et al.[22] have studied the geometric structures and electronic properties of the Pd_nCu_m ($n + m \leq 6$) clusters using DFT. The obtained results show that stability of nanoclusters of the same shape and

composition increases linearly with increasing number of PdCu bonds. Up to our knowledge, there is no report on magic number, vibrational spectra, and many body corrected electronic structure of small Pd doped Ag and Cu clusters.

In this paper, quantum mechanical calculations are employed to study pure M_n (M = Ag, Cu) and doped M_{n-m}Pd_m ($n \leq 9, m = 1, 2$) clusters and investigate the behavior of their structural, electronic, and vibrational properties as a function of size. The rest of the paper is organized as follows. In section II, we give a brief introduction of the computational method used in this work. Then in section III, atomic dimers are investigated with several exchange-correlation functional to select the proper one for our calculations. Next section involves the results of our search for lower energy structures of the selected nano-clusters. In section IV, the structural, electronic, magnetic and vibrational properties of the most stable clusters are presented. Finally, we will summarize our findings in the last section.

II. METHOD

All presented calculations are performed in the framework of the spin-polarized Kohn-Sham density functional theory by using the all electron full-potential code FHI-AIMS [23]. This package employs basis sets consisting of atom-centered numerical orbitals of the form:

$$R(r) = \frac{u_i(r)}{r} \quad (1)$$

As the name implies, the radial free atom like orbitals $u_i(r)$ are numerically tabulated and therefore exhibit very high flexibility. The strict localized nature of these basis functions lead to much slower scaling of the computational time versus the system size. The calculations reported here are done with the "tier2+spd", "tier1+spd", and "tier2" basis sets which contain 116, 152, and 45 basis functions for Cu, Ag, and Pd atoms, respectively. All the calculations were carried out in the scalar relativistic

*H. Kahnouji and H. Najafvanzadeh contributed equally to this work.

[†]Electronic address: hashemifar@cc.iut.ac.ir

limit, while the spin-orbit correction was neglected. A recent computational study on the atomic structure of transition metal clusters concluded that this relativistic term has negligible effect on the relative energy differences of the 4d systems [24].

Geometry optimization is performed by the standard Broyden-Fletcher-Goldfarb-Shanno (BFGS) algorithm [25] with a force accuracy of about $10^{-2} eV/\text{\AA}$. Harmonic frequencies are calculated using the finite displacement of all atomic positions by 10^{-3}\AA . The lowest energy structures are confirmed to be the true minima by calculating their vibrational frequencies. The FHI-aims package enables us to describe electronic single-quasiparticle excitations in molecules by using many-body correction GW self-energy [26].

III. DIMERS

First we focus on the atomic dimers to select a reliable exchange-correlation (XC) functional for our computations and moreover to gain some insights about interatomic interaction in our systems. The equilibrium bond length, binding energy, and vibrational frequency of the Cu_2 and Ag_2 dimers were calculated by using different XC approximations, including PBE [27], revPBE [28] and BLYP [29] generalized gradient (GGA) functionals and PW [30] local density functional. The obtained results are compared with available experimental data in table I. It is seen that PBE, revPBE, and BLYP give significantly more accurate binding energy and vibrational frequency while accuracy of equilibrium bond length is qualitatively the same within LDA and GGA based functionals. In the case of Cu_2 , the overall accuracy of revPBE seems to be slightly better than PBE, while the parameters of Ag_2 within PBE is overall closer to experiment. Although, BLYP gives better binding energy for Ag dimer, for larger silver clusters, other theoretical calculations [31] argue that the BLYP functional fails to predict the correct stable structure of the system. Therefore, we adapt the PBE and revPBE functionals for calculation of Ag and Cu based clusters, respectively.

For better understanding of the interatomic bonds in our target systems, we calculated the Pd_2 , CuPd , and AgPd dimers and presented their results in table I. It is observed that the bond length is increasing in the Cu_2 - CuPd - Pd_2 series while the absolute binding energy and vibrational frequency is decreasing. Hence, Cu-Cu bond has a larger strength and stiffness compared with the Cu-Pd and Pd-Pd bonds. Bond length and normal mode frequencies of AgPd and Ag_2 dimers are almost equal while these are larger than those of Pd_2 dimer. The larger bond length of Ag_2 may be due to the large atomic radius of Ag relative to Pd and Cu atoms. Binding energy of Pd_2 is smaller than that of AgPd which in turn is smaller than Ag_2 dimer.

The Mulliken population analysis of valence orbitals shows that Cu and Ag have a similar electronic configura-

TABLE I: Calculated equilibrium bond length r_e (\AA), binding energy E_b (eV/atom) and harmonic vibrational frequency ω (cm^{-1}) of the Cu_2 , Ag_2 , Pd_2 , CuPd , and AgPd dimers. The Cu_2 and Ag_2 dimers are calculated in four different exchange-correlation (XC) functionals. The corresponding experimental values (Expt.) are also given for comparison.

	XC	r_e	E_b	ω
Cu_2	PBE	2.21	-1.13	269
	BLYP	2.23	-1.11	261
	revPBE	2.24	-1.02	259
	PW	2.15	-1.39	299
	Expt.	2.21 [32]	-1.04 [33]	265 [33]
Ag_2	PBE	2.57	-0.91	180
	BLYP	2.60	-0.83	172
	revPBE	2.60	-0.79	171
	PW	2.48	-1.45	270
	Expt.	2.53 [34]	-0.83 [35]	192 [34]
CuPd	revPBE	2.32	-0.79	232
AgPd	PBE	2.56	-0.70	179
Pd_2	PBE	2.49	-0.49	195
	Expt.	2.48 [36]	-0.51 [37]	210 [38]

tion of $s^{0.94}p^{0.05}d^{10.01}$ in the Cu_2 and Ag_2 dimers. Comparing this configuration with the free Cu and Ag atoms electronic configuration ($s^1p^0d^{10}$) evidences a small *spd* hybridization in these dimers. On the other hand, comparing the electronic configuration of Pd in the Pd_2 dimer ($s^{0.58}p^{0.05}d^{9.37}$) with the free Pd atom ($s^0p^0d^{10}$) indicates a significant *spd* hybridization in the palladium dimer. The reason is that the valence shell of the free Pd atom is composed of fully occupied and fully unoccupied orbitals and hence interatomic bonding between palladium atoms requires significant promotion of electrons from the occupied *d* states to the unoccupied *s* shell. While, the valence shell of the free Cu and Ag atoms has a half filled *s* orbital which is used for interatomic bonding. It is also found that the charge transfer in the Pd-Cu and Pd-Ag bonds happens from Cu and Ag to the more electronegative Pd atom.

IV. STABLE ISOMERS

In order to investigate properties of atomic clusters, the first essential step is identification of the lowest energy structure of the clusters. Therefore, we performed a careful search for the stable structure of the pure and doped clusters. In the case of the pure clusters, all probable atomic configurations of the clusters were included in our search. After accurate atomic relaxation of the relevant configurations and comparing their minimized total energies, the most stable isomers of the pure Cu_n and Ag_n clusters ($n \leq 9$) were identified and sketched in Fig. 1. These findings are in agreement with a re-

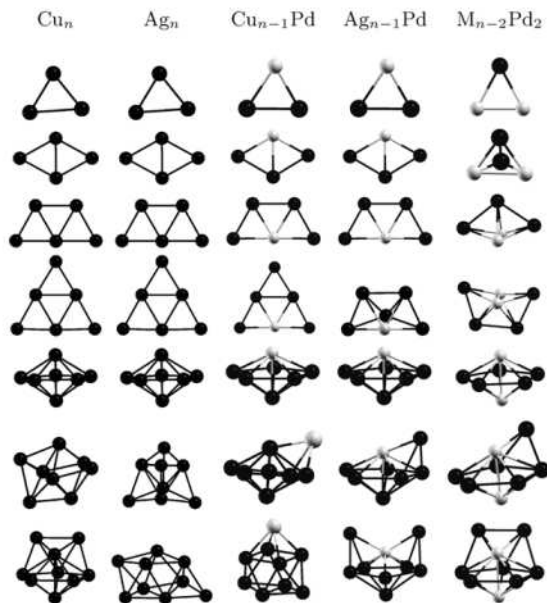


FIG. 1: Obtained lowest energy isomers of the pure Ag_n and Cu_n and doped Cu_{n-1}Pd , Ag_{n-1}Pd , $\text{Cu}_{n-1}\text{Pd}_2$, and $\text{Ag}_{n-1}\text{Pd}_2$ clusters for $3 \leq n \leq 9$. The Pd atoms are shown by light balls while the Cu/Ag atoms are indicated by black balls.

cent study on silver clusters [39]. Because of the presence of two different atoms, the process of finding the global minimum energy structure of the doped clusters is more complicated than the pure clusters. Therefore, for finding the most stable structures of the palladium doped clusters, we tried to limit our search to the more stable configurations proposed by previous studies on the Cu_nPd_m ($n+m \leq 6$) [22] and Ag_nPd_m ($n+m \leq 5$) [20, 40] clusters. The resulting most stable isomer of the doped clusters are presented in Fig. 1. It is seen that the most stable $\text{M}_{n-2}\text{Pd}_2$ clusters are made of the maximum number of pyramids and moreover the two Pd atoms in these systems tend to bond together. These observations were used for obtaining the most stable structure of the M_6Pd_2 and M_7Pd_2 clusters.

The results show that up to the size of 6 (heptamer), pure clusters prefer 2 dimensional (2D) planar structures while larger clusters stabilize in 3D geometries. In order to understand the origin of this 2D-3D cross over, we analyzed the average bond length (d) and the average coordination number of atoms (n_c) in the most stable 2D and 3D isomers of the Cu_n and Ag_n clusters (Fig. 2). It is seen that the 2D isomers have lower average coordination and shorter average bond length, because the valence charge density of these systems is distributed among lower number of bonds, compared with the 3D isomers. As a result of that, individual bonds in the planner isomers are stronger and shorter, while 3D isomers have more number of bonds. The 2D-3D structural

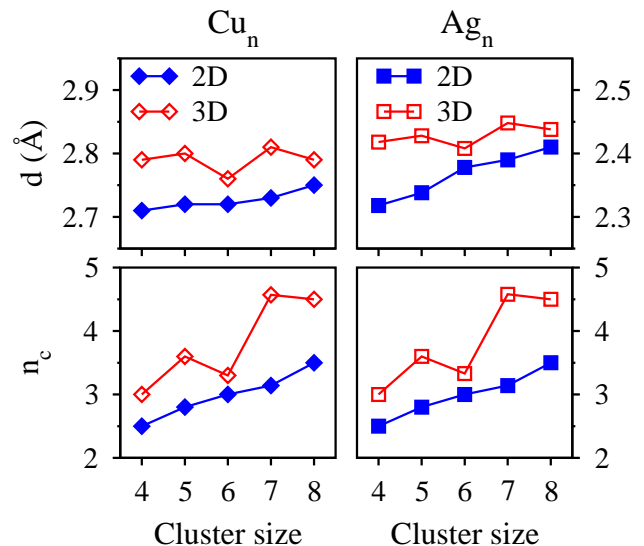


FIG. 2: Average bond length d and coordination number of atoms n_c in the most stable 2D and 3D structures of Cu_n (left) and Ag_n (right) clusters.

transformation reflects the competition between the individual bond strength and the total number of bonds. It is observed that (Fig. 2) in the smaller sizes ($n \leq 6$), the more pronounced difference in the individual bond strength leads to the stability of the 2D isomers, while for the larger clusters the difference in the average coordination wins the competition and stabilizes the 3D isomers.

The results (Fig. 1) indicate that the most stable 2D isomers of Cu_n and Ag_n clusters are made of equilateral triangles. It is also seen that the 2D-3D cross over in the Ag_{n-1}Pd clusters occurs at $n = 6$ while the Cu_{n-1}Pd clusters, follow the same structural transformation as the pure Cu cluster. As a general trend, we observe that the Pd atom prefers the high coordinated sites of the Cu_{n-1}Pd and Ag_{n-1}Pd clusters. The obtained results indicate high tendency of the $\text{M}_{n-2}\text{Pd}_2$ clusters toward 3D configurations. Considering various 2D and 3D structures for the M_2Pd_2 , it was found that the 3D structures have lower energies, in agreement with the previous works [22, 40]. Based on these results, the theoretical search for the stable isomers of the $\text{M}_{n-2}\text{Pd}_2$ clusters were limited to all 3D isomers of the pure Ag and Cu clusters. It is worth while to mention that other authors have not investigated $\text{Cu}_{n-2}\text{Pd}_2$ and $\text{Ag}_{n-2}\text{Pd}_2$ clusters larger than five and six atoms, respectively.

V. STRUCTURAL PROPERTIES

In order to address stability and structural behaviour of the clusters, the binding energy per atom, average coordination number of atoms, and the average bond length of the most stable structures of all clusters under study as a function of the cluster size are presented in Fig.

3. The harmonic vibrational frequencies of the clusters were also calculated to address dynamical stability and bond stiffness of the systems. The maximum vibrational frequency of the clusters are shown in Fig. 3. The calculated binding energy of the copper clusters are in well agreement with the measured data. It can be seen that by increasing the cluster size, the binding energy of the pure clusters increases gradually toward the binding energy of bulk copper (3.50 eV)[41] and silver (2.95 eV)[41], although these clusters are clearly far from the bulk limit. Notably, the eight atom pure clusters occurs in a local maximum of the absolute binding energy. It is clearly seen that the 2D to 3D structural transformation in the pure and mono-doped clusters is reasonably accompanied by a sharp increases in the average coordination number of atoms.

Observation of no imaginary frequency indicates the dynamical stability of the lowest energy isomers shown in Fig. 1. It is generally seen that the Ag based clusters have lower vibrational frequency than Cu based clusters, which is clearly related to the higher atomic mass of silver. Considering the trend of maximum frequencies along with the geometry of the most stable isomers of the clusters (Fig. 1) clarifies that the structural cross over from planar to 3D geometries in the pure Ag and Cu clusters and doped Cu_{n-1}Pd cluster is accompanied with a significant mode softening in the vibrational spectra.

Comparing the properties of the pure and doped clusters show that Pd doping in the copper clusters increases the average bond length of the system, because of the larger atomic radius of Pd compared with Cu. This increase is expected to be accompanied by a bond softening effect, which is generally visible in the calculated harmonic vibrational frequency of the doped Cu clusters. In contrast to this bond elongating and softening effects, we observe that Pd doping has a weak effect on the binding energy of Cu clusters. It seems that the doped Pd atom in the Cu cluster, inserts effective amount of electrons in the neighboring bonds and hence compensate the observed bond softening effects. It is reasonable, because Pd has much more electrons than Cu. On the other hand, the average bond length of the doped Ag clusters is slightly smaller than those of the pure clusters. The reason is that atomic size of silver is larger than that of palladium and hence Ag-Pd and Pd-Pd bonds are shorter than Ag-Ag one (table I). As a result of that, a bond hardening effect is visible in the calculated vibrational spectra of the doped Ag clusters, compared with the pure ones. As a result of these bond shortening and hardening effects, Pd doping enhances the absolute binding energy of Ag clusters (Fig. 3).

In cluster science, the second-order energy difference ($\Delta_2 E$) is a conventional quantity to address the relative stability of clusters as a function of size and reproduce the experimental magic numbers observed in mass spectra measurements. Large values of $\Delta_2 E(n)$ indicate that the n -atoms cluster is more stable than $n-1$ and $n+1$ atoms

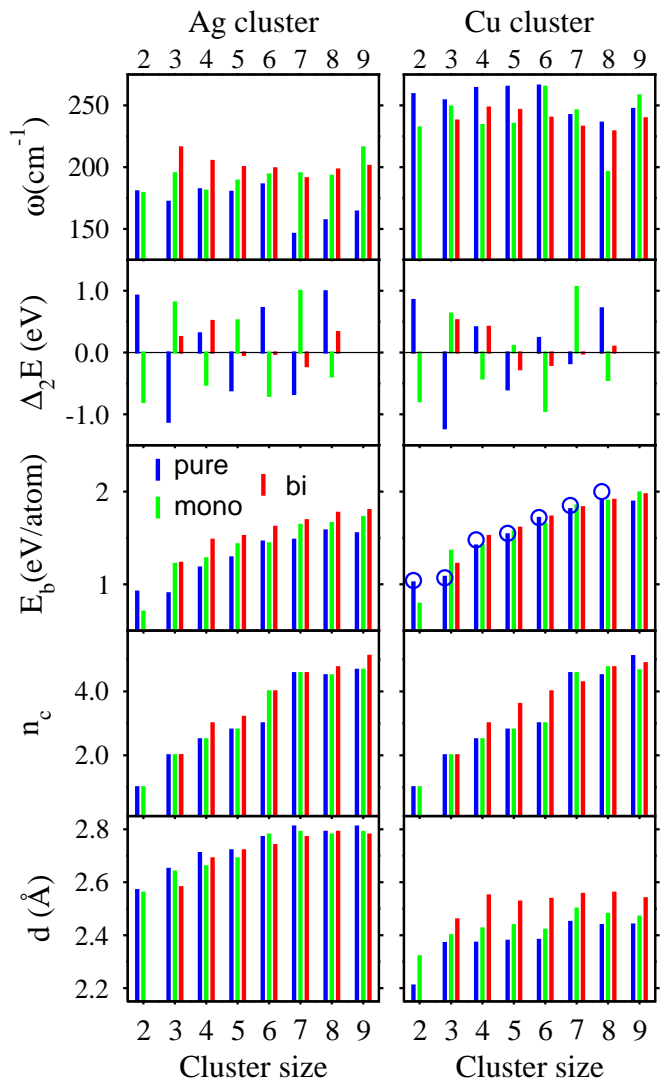


FIG. 3: Calculated maximum vibrational frequency (ω), Second difference of the energy $\Delta_2 E(n)$, absolute binding energy per atom E_b , average coordination number of atoms n_c , and the average bond length d of the pure, mono-doped, bi-doped Ag and Cu clusters as a function of size. The empty circles show the measured binding energy of the pure Cu clusters [42].

clusters. This parameter is defined as follows:

$$\Delta_2 E(n) = E_{tot}(n+1) + E_{tot}(n-1) - 2E_{tot}(n) \quad (2)$$

$E_{tot}(n)$ is the minimized energy of the $M_{n-m}\text{Pd}_m$ cluster ($M = \text{Ag}, \text{Cu}$) and $E_{tot}(n+1)$ ($E_{tot}(n-1)$) is the minimized energy of the cluster with one more (less) M atom. The calculated second-order energy difference of the pure and doped Cu and Ag clusters is plotted in Fig. 3. It is seen that pure clusters show strong peaks at $n = 2, 8$ which indicate the highest relative stability of these systems and propose $n = 2, 8$ as the first magic numbers of small pure Ag and Cu clusters, in agreement with the experimental observations [43–46] and electronic

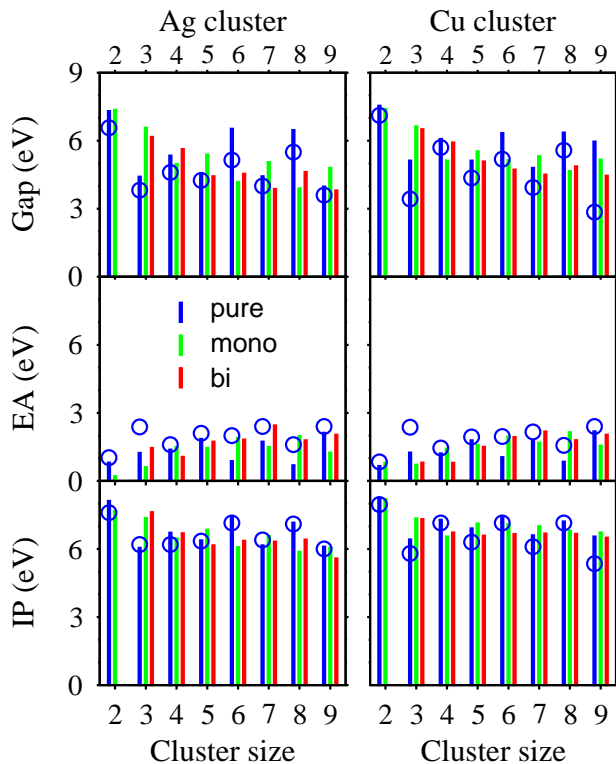


FIG. 4: Calculated HOMO-LUMO gap, Ionization potential (IP), and electron affinity (EA) of the pure, mono-doped, and bi-doped Ag (left column) and Cu clusters (right column) after the GW correction. The empty circles show the available measured data for pure clusters, collected from references [49–54].

shell jellium model [47, 48]. The predicted magic numbers for mono-doped clusters are 3 and 7, while in the case of bi-doped clusters, the main peaks are observed at $n = 3, 4, 8$.

Furthermore, a clear odd-even oscillation is seen in the pure and mono-doped clusters, although bi-doped clusters do not display such clear oscillations. It is worthwhile to mention that electron pairing in HOMO can explain this oscillations and the more stability of the even pure and odd mono-doped clusters. The valence electrons of the pure M_n and mono-doped $M_{n-1}Pd$ clusters are mainly composed of the M s electrons, hence clusters with odd number of M atoms have one unpaired electron and consequently exhibit lower stability. The pure and mono-doped clusters with even number of M atoms have a close electronic shell and hence are more stable. On the other hand, the behaviour of the Δ_2E curve of the bi-doped clusters is more complicated and needs to further arguments. We attribute this more complicated behaviour to the effective contribution of d electrons to the valence shell of the bi-doped clusters. As it was argued in section III, the direct bonding between Pd atoms in the bi-doped clusters give rises to effective promotion of the Pd d electrons to the valence shell of the system.

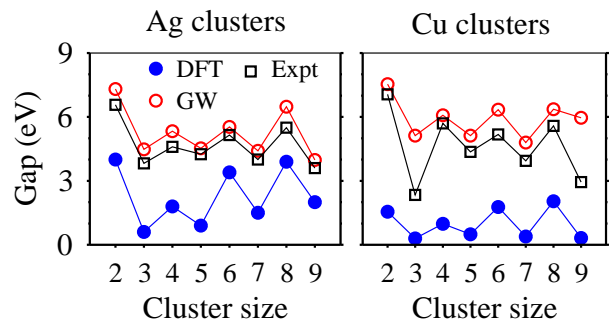


FIG. 5: Calculated HOMO-LUMO gap of the pure Ag and Cu clusters before and after the GW correction along with the available experimental data, collected from references [49–54].

VI. ELECTRONIC PROPERTIES

Since the single particle Kohn-Sham eigenvalues have no clear physical meaning, the reliable energy level of the highest occupied (HOMO) and the lowest unoccupied molecular orbital (LUMO) of the clusters are determined after applying the many-body GW perturbation theory [26]. The GW corrected HOMO and LUMO energies are expected to be comparable to the experimental ionization potential (IP) and electron affinity (EA) of the clusters. These values along with the computed HOMO-LUMO gaps are presented in Fig. 4. The available measured data for pure clusters are also presented in this figure. The calculated values of IP and Gap exhibit good agreement with the experimental data which is mainly due to the GW correction, while the calculated EA values in some cases are considerably overestimated. In order to show the effect of this many body correction, we have compared in Fig. 5 the experimental values of the HOMO-LUMO gap of the pure clusters with the calculated ones before and after application of the GW correction. It is seen that the Kohn-Sham gaps are significantly underestimated while the GW corrected gaps are generally much closer to experiment. The observed odd-even oscillations in the IP and EA of the pure clusters are attributed to the electron pairing in these systems, discussed in the previous section. The lower value of EA for even clusters indicates less tendency of these closed shell systems to receive an extra electron, compared with the open shell clusters. A consistent reversed trend is visible in the obtained ionization potentials.

In the same way, the ionization potential and electron affinity of the most stable structure of the doped clusters were calculated and displayed in Fig. 4. The higher value of IP for the odd $M_{n-1}Pd$ clusters indicates their more chemical stability compared to the neighboring even clusters. In the bi-doped clusters, the IP and EA curves do not show clear oscillations with respect to cluster sizes, which is likely due to the effective contribution of d electrons to the Pd-Pd bonding in these clusters. The trend of the calculated HOMO-LUMO gap is generally consistent with the Δ_2E , indicating that the systems with

higher gap are generally more stable. It is consistent with the chemical intuition that a higher value of the HOMO-LUMO gap indicates less chemical activity and hence more stability. Considering the spin polarized electronic structure of the most stable isomers, we found out that consistent with the simple spin pairing rule, all studied clusters prefer the lowest possible spin multiplicity. Hence, the pure and doped clusters with even number of Ag and Cu atoms are nonmagnetic while others exhibit a total spin moment of $1 \mu_B$.

VII. CONCLUSIONS

In this paper, spin-polarized all-electron calculations were performed to investigate structural and electronic properties of the pure and Pd doped Cu_n and Ag_n clusters ($n \leq 9$). It was argued that a 2D to 3D structural cross over occurs in the size of seven of the pure clusters. The magic numbers of the pure clusters were found to be 2 and 8. The obtained results indicate that the doped Pd atoms generally prefer the high coordinated sites of the pure clusters. We found that the magic numbers of the mono-doped clusters are 3 and 7 while bi-doped clusters

exhibit magic numbers 3, 4, and 8. It was argued that doping with one Pd atom slightly reduces the onset of the 2D to 3D structural crossover of the pure Ag clusters, while doping with two Pd atoms strongly enhances stability of the 3D isomers and completely destroys this cross over. Moreover, it was observed that the bond stiffness of the Cu clusters are decreased after doping with Pd atoms while their average bond strength have lower sensitivity to doping. On the other hand, Pd doping increases the bond stiffness and bond strength of the Ag clusters. It was discussed that electron pairing in the HOMO, induces a significant odd-even fluctuation in the ionization potential, electron affinity, and HOMO-LUMO gap of the pure Ag and Cu clusters, while doping with Pd atoms considerably weakens this fluctuation.

Acknowledgments

This work was jointly supported by the Vice Chancellor for Research Affairs of Isfahan University of Technology (IUT), Centre of Excellence for Applied Nanotechnology, and ICTP Affiliated Centre at IUT.

-
- [1] T. Udayabhaskararao and T. Pradeep, J. Chem. PhysLett. **4**, 1553 (2013).
- [2] M. C. Daniel and D. Astruc, Chem. Rev **104**, 293 (2004).
- [3] C. Burda, X. Chen, R. Narayanan, and M. A. El-Sayed, Chem. Rev. **105**, 1025 (2005).
- [4] C. J. Murphy, A. M. Gole, S. E. Hunyadi, and C. J. Orendorff, Inorg.Chem **45**, 7544 (2006).
- [5] Y. Xia, P. D. Yang, Y. G. Sun, Y. Y. Wu, B. Mayers, B. Gates, F. K. Y. D. Yin, and Y. Q. Yan, Adv. Mater. **15**, 353 (2003).
- [6] A. X. Trautwein, *Bioinorganic Chemistry* (Wiley-VCH, Weinheim, 1997).
- [7] G. Aragay, J. Pons, and A. Merkoci, Chem. Rev **111**, 3433 (2011).
- [8] M. Neergat, A. Shukla, and K. Gandhi, J. Appl. Electrochem **31**, 373 (2001).
- [9] W. Li, W. Zhou, H. Li, Z. Zhou, B. Zhou, G. Sun, and Q. Xin, Electrochim. Acta **49**, 1045 (2004).
- [10] B. Anak, M. Bencharif, and F. Rabilloud, RSC Adv. **4**, 13001 (2014).
- [11] M. Deshpande, D. Kanhere, I. Vasiliev, and R. Martin, Phys. Rev. B **68**, 0345428 (2003).
- [12] E. M. Fernandez, J. M. Soler, I. L. Garzn, and L. C. B. ., Phys. Rev. B. **70**, 165403 (2004).
- [13] R. Fournier, J. Chem. Phys **115**, 2165 (2001).
- [14] W.Su, P.Qian, Y.Liu, J.Shen, and N.X.Chen, Comput.Phys.Commun **181**, 726 (2010).
- [15] A. Prestianni, A. Martorana, F. Labat, I. Ciofini, and C. Adamo, J. Mol. Struct.: THEOCHEM **3**, 903 (2009).
- [16] W. Bouderbala and A.GhaniBoudjahem, Physica B **454**, 217 (2014).
- [17] M. Wang, X. Liu, J. Meng, and Z. Wu, J. Mol. Struct. THEOCHEM **4**, 802 (2007).
- [18] S. Romanowski, W. Bartczak, and R. Wesokowski, Langmuir **15**, 5773 (1999).
- [19] M. N. F. Gobal, R. Arab, Journal of Molecular Structure: THEOCHEM **959**, 15 (2010).
- [20] D. Kilimis and D. Papageorgiou, Journal of Molecular Structure: THEOCHEM **939**, 112 (2010).
- [21] S. Zhao, Y. Ren, Y. Ren, J. Wang, and W. Yin, International journal of Quantum chemistry **111**, 232 (2428).
- [22] I. Efremenko and M. Sheintuch, Chem. Phys. Lett. **401**, 232 (2005).
- [23] V. Blum and M. Scheffler and R. Gehrke and F. Hanke and P. Havu and X. Ren and K. Reuter, The Fritz Haber Institute ab initio molecular simulation package (FHI-aims) 2009, <http://www.fhi-berlin.mpg.de/aims>.
- [24] M. Piotrkowski and P. P. J. D. Silva, Phys. Rev. B **81**, 1554461 (2010).
- [25] W. Press, S. Teukolsky, W. Vetterlin, and B. Flannery, *NumericalRecipes:The ArtofScientific Computing* (Cambridge University Press., 2007).
- [26] M. Schilfgaardel, T. Kotani, and S. Faleev, Phys. Rev. Lett **96**, 226402 (2006).
- [27] J. Perdew, K. Burke, and M. Ernzerhof, Phys. Rev. Lett. **77**, 3865 (1996).
- [28] B. Hammer, PHYSICAL REVIEW B **59**, 7414 (1999).
- [29] D. Becke, Phys. Rev. A **38**, 3098 (1988).
- [30] J. P. Perdew and Y. Wang, Phys. Rev. B **45**, 13244 (1992).
- [31] S. Zhao, Z. Li, W.-N. Wang, Z. Liu, and K. .Fan, J. Chem. Phys. **124**, 184102 (2006).
- [32] R. Ram, C. Jarman, and P. Bernath, J. Mol. Spectrosc. **156**, 468 (1992).
- [33] M. Mors, *Advances in Metal and Semiconductor Clusters* (JAI Press, Greenwich, CT, 1993).

- [34] B. Simard, P. Hackett, A. James, and P. LangridgeSmith, *Chem. Phys. Lett* **186**, 415 (1991).
- [35] M. Morse, *Chem. Rev* **86**, 1049 (1986).
- [36] K. Huber and G. Herzberg, *Molecular Spectra and Molecular Structure. IV. Constants of Diatomic Molecules* (Van Nostrand Reinhold Company, New York, 1979).
- [37] I. Shim and K. Gingerich, *J. Chem. Phys* **80**, 5107 (1984).
- [38] J. Ho, M. Polak, K. Ervin, and W. Lineberger, *J. Chem. Phys* **99**, 8542 (1993).
- [39] M. Harb, F. Rabilloud, D. Simon, A. Rydlo, S. Lecoultré, F. Conus, V. Rodrigues, and C. Flix, *J. Chem. Phys* **129**, 194108 (2008).
- [40] S. Zhao, Y. Ren, Y. Ren, J. Wang, and W. Yin, *Computational and Theoretical Chemistry* **964**, 298 (2011).
- [41] C. Kittel, *Introduction to Solid State Physics* (Wiley, New York, 2005).
- [42] V. Spasov, T. Lee, and K. Ervin, *J. Chem. Phys.* **112**, 1713 (2000).
- [43] V. A. Spasov, T.-H. Lee, and K. M. Ervin, *J. Chem. Phys* **112**, 1713 (2000).
- [44] O. Ingolfsson, U. Busolt, and K. Sugawara, *J. Chem. Phys* **112**, 4613 (2000).
- [45] Katakuse, T. Ichihara, Y. Fujita, T. Matsuo, T. Sakurai, and H. Matsuda, *Int. J. Mass Spectrom. Ion Process* **65**, 229 (1985).
- [46] Katakuse, T. Ichihara, Y. Fujita, T. Matsuo, T. Sakurai, and H. Matsuda, *Int. J. Mass Spectrom. Ion Process* **74**, 33 (1986).
- [47] M. Brack, *Rev. Mod. Phys.* **65**, 677 (1993).
- [48] W. de Heer, *Rev. Mod. Phys.* **65**, 611 (1993).
- [49] C. Jackschath, I. Rabin, and W. Schulze, *Z. Phys. D: At., Mol. Clusters.* **22**, 517 (1992).
- [50] V. A. Spasov, T. Lee, J. Maberry, and K. Ervin, *J. Chem. Phys.* **110**, 5208 (1999).
- [51] D. Leopold, J. Ho, and W. Lineberger, *J. Chem. Phys.* **86**, 1715 (1987).
- [52] K. Ervin, J. Ho, and W. Lineberger, *J. Chem. Phys.* **93**, 6987 (1990).
- [53] M. B. Knickelbein, *Chem. Phys. Lett.* **192**, 129 (1992).
- [54] D. Powers, S. Hansen, M. Geusic, D. Michalopoulos, and R. Smalley, *J. Chem. Phys.* **78**, 2866 (1982).